

Subradiant split Cooper pairs

Audrey Cottet¹, Takis Kontos¹ and Alfredo Levy Yeyati²

¹Laboratoire Pierre Aigrain, Ecole Normale Supérieure, CNRS UMR 8551, Laboratoire associé aux universités Pierre et Marie Curie et Denis Diderot, 24, rue Lhomond, 75231 Paris Cedex 05, France and

²Departamento de Física Teórica de la Materia Condensada C-V and Instituto Nicolás Cabrera, Universidad Autónoma de Madrid, E-28049 Madrid, Spain

We suggest a way to characterize the coherence of the split Cooper pairs emitted by a double-quantum-dot based Cooper pair splitter (CPS), by studying the radiative response of such a CPS inside a microwave cavity. The coherence of the split pairs manifests in a strongly nonmonotonic variation of the emitted radiation as a function of the parameters controlling the coupling of the CPS to the cavity. The idea to probe the coherence of the electronic states using the tools of Cavity Quantum Electrodynamics could be generalized to many other nanoscale circuits.

Entanglement is now accepted as an intriguing but available resource of the quantum world. However, it is still unclear whether this phenomenon can survive in nanoscale electronic circuits, because an electronic fluid is characterized by a complex many-body state in general. Producing and detecting entangled electronic states are therefore important goals of quantum electronics. The spin-singlet (Cooper) pairing of electrons, naturally present in conventional superconductors, appears as a very attractive source of electronic entangled states. Recently, the splitting of Cooper pairs could be demonstrated in Y-junctions made out of nanowires [1–3]. But how to distinguish between a singlet state broken into a product state due to decoherence and the desired coherent singlet state is not addressed in these experiments. Here, we show that the radiative response of such devices can reveal the presence or absence of entangled states. The split Cooper pairs are shown to decouple from the electromagnetic field conveyed by a photonic cavity (subradiance) if coherent. These findings add a new twist to quantum opto-electronics, and could be applied to any source of on-demand entangled electronic states.

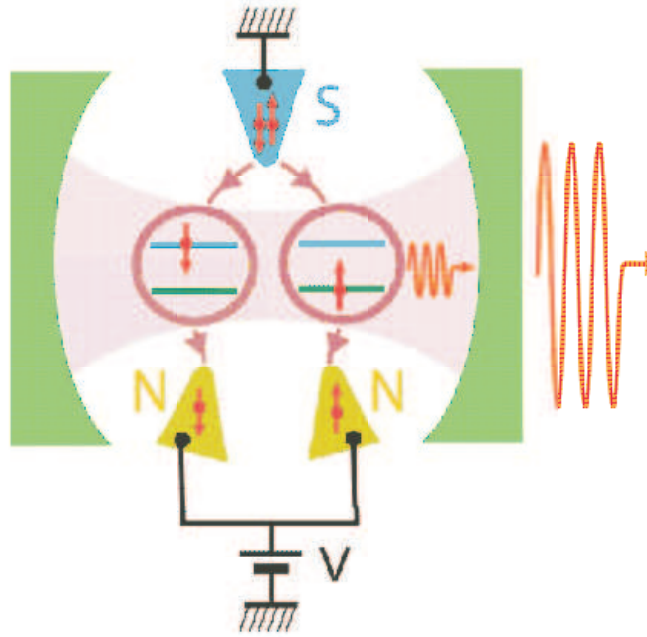


FIG. 1: Scheme of the CPS embedded in a photonic cavity. The CPS is made out of a double quantum dot coupled to a central blue superconducting contact (S) connected to ground, and two outer yellow normal metal contacts (N) biased with a voltage V . This circuit is placed inside a photonic cavity (represented schematically by mirrors in green). The Cooper pairs spread over the K and K' orbitals of the dots, sketched in blue and green respectively. The low energy level structure of the system allows photon emission which can be amplified through a lasing effect.

The analogy between a beam splitter for electronic states and a beam splitter for photons calls for the use of corre-

lation measurements to characterize the degree of entanglement of pairs of electrons, via the noise cross-correlations of the electrical current [4–10]. The use of a double quantum dot circuit connected to two normal electrodes and one superconducting electrode gives a practical realization of an electronic entangler and simplifies the diagnosis of entanglement from transport, as originally suggested by Recher et al. [7]. Nevertheless, measuring cross-correlations in such a setup is a formidable task because the conditions for useful entanglement correspond to a regime where the system is almost isolated from the leads. In this case, the Cooper pair current is too small to yield measurable current fluctuations with present amplification techniques [11]. These difficulties stem from the fact that probing directly a quantum system with transport measurements is not natural since one needs the system to be open and closed at the same time. On the contrary, as known in atomic physics [12], the use of light-matter interaction is very well adapted to probe closed quantum systems. Here, we show how to use the coupling between electrons and photons from a microwave cavity, to assess the coherence of Cooper pairs emitted by a CPS implemented with a double quantum dot circuit.

We consider a CPS made out of a single wall carbon nanotube in which a double dot is defined by a central superconducting contact connected to ground and two outer normal metal contacts biased with a voltage V . This CPS is inserted inside a photonic cavity (see Figure 1) which is assumed to be implemented in a coplanar waveguide geometry using a superconducting metal, like in the Circuit Quantum Electrodynamics architecture [13]. Very recently, it has been demonstrated experimentally [14, 15] that one can extend this architecture to quantum dot circuits [16–19], bringing our proposed

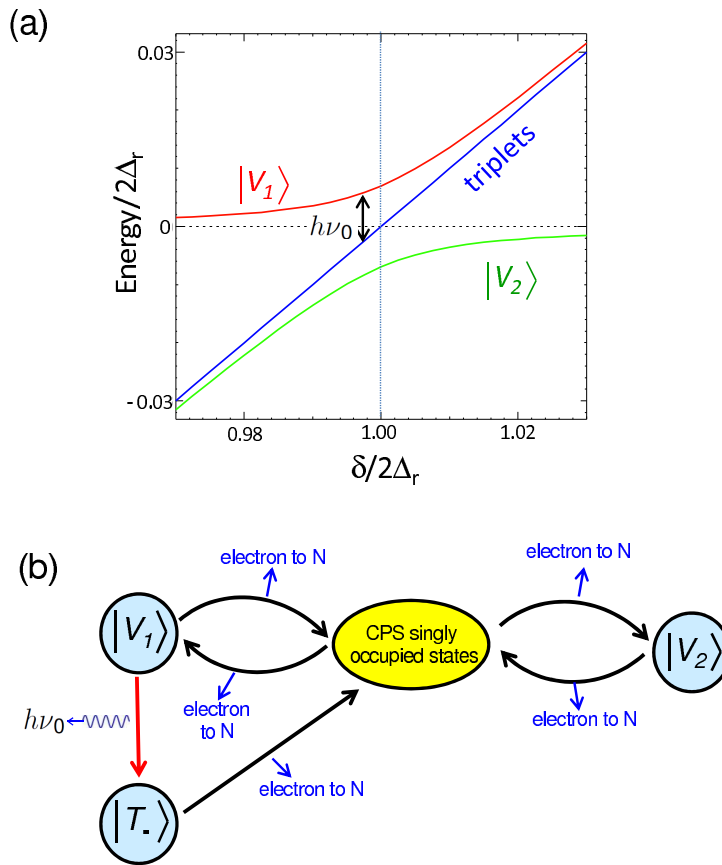


FIG. 2: a. Spectrum of the subset \mathcal{E} of even charge states of the CPS near $\delta = 2\Delta_r$. It comprises three spin-triplet states, and two states $|V_1\rangle$ and $|V_2\rangle$ which are a coherent mixture of the empty state and a spin-singlet state $|S\rangle$. b. Dynamics of the CPS near the working point $\delta = 2\Delta_r$. We consider a bias voltage regime such that the various transitions between the CPS states occur together with the transfer of one electron towards the normal contacts, apart from the transition from $|V_1\rangle$ to the triplet state $|T_-\rangle$, which occurs due to the emission of a photon towards the cavity. We have checked that the radiative transition from $|T_-\rangle$ to $|V_2\rangle$ is not active in the regime of parameters we consider.

Our aim is to find an effect which reveals qualitatively the coherent injection of Cooper pairs. Thanks to Coulomb blockade, the states participating to electronic transport can be reduced to the double-dot empty state $|0, 0\rangle$, the

singly occupied states $|\tau\sigma, 0\rangle = d_{L\tau\sigma}^\dagger |0, 0\rangle$ and $|0, \tau\sigma\rangle = d_{R\tau\sigma}^\dagger |0, 0\rangle$ of the left (L) and right (R) dot, and the non-local doubly occupied states $|\tau\sigma, \tau'\sigma'\rangle = d_{L\tau\sigma}^\dagger d_{R\tau'\sigma'}^\dagger |0, 0\rangle$, with $\tau \in \{K, K'\}$ and $\sigma \in \{\uparrow, \downarrow\}$ being orbital and spin indices respectively (see Supplemental Material (SM), part A for details). For biasing conditions like the one depicted in Fig. 1 with $eV < \Delta$ (Δ being the gap of the superconducting contact) Cooper pairs are injected from the superconductor into a singlet state $|\mathcal{S}\rangle$. The coupling to the superconductor hybridizes the $|\mathcal{S}\rangle$ state with the empty state $|0, 0\rangle$ forming two states which we call $|V_1\rangle$ and $|V_2\rangle$. These states can relax to a single particle state via electron tunneling into the normal leads, and then via a second tunneling process into the state $|V_1\rangle$ or $|V_2\rangle$, which closes the usual operation loop of the CPS, as depicted in Fig. 2b. However, when the CPS is placed in the resonant cavity there is an additional transition to a triplet state (two electronic states with equal spin) through the emission of a cavity photon. It is the aim of this work to study these photon emission processes and show that they can be used to characterize the coherence of the split pairs injected into the CPS.

The relevant energy scales of the CPS are the position ε of the energy levels on each dot, which we assume symmetric for the sake of simplicity, the Cooper pair coherent splitting rate t_{eh} [20, 21], the effective spin-orbit coupling constant Δ_{so} and the coupling between the K and K' orbitals, $\Delta_{K\leftrightarrow K'}$, which arise from weak disorder in the nanotube [22–25]. For $t_{eh} = 0$, $\Delta_{so} = 0$, and $\Delta_{K\leftrightarrow K'} = 0$, the doubly occupied states cost an energy $2\varepsilon = \delta$. For $t_{eh} \ll \Delta_{K\leftrightarrow K'}, \Delta_{so}$ [1], the regime $\delta \sim 2\Delta_r$, with $\Delta_r = \sqrt{\Delta_{so}^2 + \Delta_{K\leftrightarrow K'}^2}$, is the most adequate for producing entangled states. It allows one to isolate, in the double dot even charge sector, a subset \mathcal{E} of five lowest energy eigenstates which are at a distance $\sim 2\Delta_r$ from the other even charge states, at least. These five states include three spin-triplet states $|T_0\rangle$, $|T_+\rangle$, and $|T_-\rangle$ with energy $E_{triplet} = \delta - 2\Delta_r$ and the two hybridized even states [26, 27] $|V_n\rangle = \sqrt{1 - v_n^2}|0, 0\rangle + v_n|\mathcal{S}\rangle$ with energy $E_i = \frac{1}{2} \left(\delta - 2\Delta_r - (-1)^n \sqrt{8t_{eh}^2 + (\delta - 2\Delta_r)^2} \right)$ for $n \in \{1, 2\}$ (see SM, part B.4, for the expression of the $v'_n s$). Here, the definition of the spin-singlet state $|\mathcal{S}\rangle$ and the spin-triplets take into account the twofold orbital degeneracy of each dot (see SM, part B.4). The energies of $|V_1\rangle$ and $|V_2\rangle$ show an anticrossing with a width $E_p = 2\sqrt{2}t_{eh}$ at $\delta = 2\Delta_r$, while the energy of the triplets lies in the middle (see Figure 2.a).

Let us first discuss the current I_{CPS} through the superconducting lead, without considering the effect of the photonic cavity. We call Γ_N the bare tunnel rate of an electron between one dot and the corresponding normal metal contact, while P_A denotes the probability of a state $|A\rangle$ of the double dot even charge sector and P_{single} the global probability of having a double dot singly occupied state. In the sequential tunneling limit $\Gamma_N \ll k_B T$, these probabilities follow a master equation $\frac{d}{dt}P = M P$ with

$$P = \begin{bmatrix} P_{V_1} \\ P_{V_2} \\ P_{T_-} \\ P_{single} \end{bmatrix}, \quad \frac{M}{\Gamma_N} = \begin{bmatrix} -2v_1^2 & 0 & 0 & 1 - v_1^2 \\ 0 & -2v_2^2 & 0 & 1 - v_2^2 \\ 0 & 0 & -2 & 0 \\ 2v_1^2 & 2v_2^2 & 2 & -1 \end{bmatrix} \quad (1)$$

Equation (1) corresponds to a bias voltage regime such that single electrons can go from the double dot to the normal leads but not the reverse (see SM, part C). We disregard the states $|T_0\rangle$ and $|T_+\rangle$, which are not populated in the simple limit we consider. The states $|V_i\rangle$ and $|T_-\rangle$ can decay towards several different singly occupied states. The sum of the corresponding transition rates equals $2\Gamma_N v_i^2$ and $2\Gamma_N$ respectively, which explains the presence of the factors 2 in the 3 first columns of M . To calculate I_{CPS} , one first has to determine the stationary value P_{stat} of P from $M P_{stat} = 0$. Then, one can use $I_{CPS} = R \cdot P_{stat}$ with $R = e\Gamma_N[2v_1^2, 2v_2^2, 2, 1]$. If the double dot is initially in the state $|V_n\rangle$, with $n \in \{1, 2\}$, there can be a transition to a singly occupied state while an electron is transferred to the normal leads, because $|V_n\rangle$ has a $|\mathcal{S}\rangle$ component. Then, there can be a transition from this singly occupied state to $|V_m\rangle$, with $m \in \{1, 2\}$, because $|V_m\rangle$ has a $|0, 0\rangle$ component. This leads to the existence of state cycles which produce a flow of electrons towards the normal leads (see Figure 2.b). On the left(right) of the anticrossing point $\delta = 2\Delta_r$, the state $|V_{1(2)}\rangle$ is the most probable. Exactly at the anticrossing point, the states $|V_1\rangle$ and $|V_2\rangle$ contribute equally to current transport and I_{CPS} is maximum (see Fig.3, main frame).

Electronic spins are naturally coupled to photons thanks to the spin-orbit interaction, which exists in many types of conductors, including those used to demonstrate Cooper pair splitting. In our case, we will take into account a spin/photon coupling with the form (see SM, part F)

$$H_{so} = (a + a^\dagger) \sum_{i, \tau, \sigma} \lambda_{i\sigma} d_{i\tau\sigma}^\dagger d_{i\tau\bar{\sigma}} = (a + a^\dagger) h_{so} \quad (2)$$

with $d_{i\tau\sigma}^\dagger$ the creation operator for an electron with spin σ in orbital τ of dot $i \in \{L, R\}$ and a^\dagger the creation operator for cavity photons. We use $\lambda_{i\sigma} = \mathbf{i}\sigma\lambda_i$. Inside the \mathcal{E} subspace, the term H_{so} couples $|V_n\rangle$ to $|T_-\rangle$ only, i.e., for

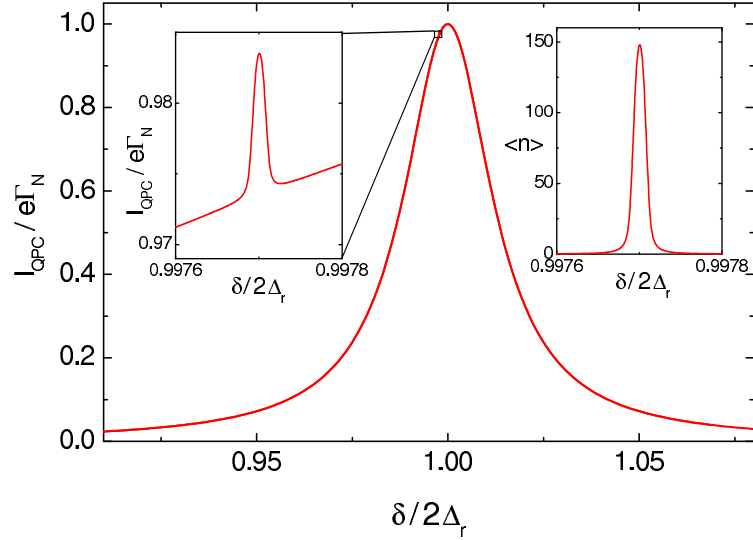


FIG. 3: Main frame: Current I_{QPC} at the input of the Cooper pair splitter. The peak at $\delta = 2\Delta_r$ is due to the anticrossing between $|V_1\rangle$ and $|V_2\rangle$. Left inset: zoom on the current peak due to lasing transitions between the $|V_1\rangle$ and $|T_-\rangle$ states. Right inset: number of photons versus δ . We have used realistic parameters $t_{eh} = 9 \mu\text{eV}$, $\Delta_{so} = 0.15 \text{ meV}$, $\Delta_{K/K'} = 0.9 \text{ meV}$, $\nu_0 = 3.64 \text{ GHz}$, $Q = 2\pi\hbar\nu_0/\kappa = 500000$, $D_{pq}^{-1} = 92 \text{ ns}$, $\Gamma_N = 72 \text{ MHz}$, $T = 35 \text{ mK}$, and $|\lambda_L - \lambda_R| = 2.5 \cdot 10^{-6} \Delta_r \simeq 0.55 \text{ MHz}$.

$n \in \{1, 2\}$,

$$\langle T_- | h_{so} | V_n \rangle = \mathbf{i}v_n \frac{\Delta_{K \leftrightarrow K'}}{\Delta_r} (\lambda_L - \lambda_R) \quad (3)$$

whereas $\langle T_{+[0]} | h_{so} | V_{1(2)} \rangle = 0$. The presence of the minus sign in Eq.(3) is crucial. It reveals the *coherent* injection of singlet pairs inside the CPS. If $|V_n\rangle$ was resulting from the hybridization of a product spin state with the $|0,0\rangle$ state, the matrix element (3) would depend only on λ_L or λ_R . We will show below that the peculiar structure of the element (3) can be revealed by measuring the lasing effect associated to the transition $|V_1\rangle \rightarrow |T_-\rangle$.

In order to study current transport and the photonic dynamics simultaneously, one can generalize the above master equation description by using a semi-quantum description of lasing [28]. This consists in adding inside the matrix M rates accounting for photonic emission and absorption processes, i.e. $M \rightarrow M + M_{ph}$ with

$$M_{ph} = \begin{bmatrix} 0 & 0 & W_{V_1 T_-} & 0 \\ 0 & -W_{T_- V_2} & 0 & 0 \\ 0 & W_{T_- V_2} & -W_{V_1 T_-} & 0 \\ 0 & 0 & 0 & 0 \end{bmatrix} \langle n \rangle + \begin{bmatrix} -W_{V_1 T_-} & 0 & 0 & 0 \\ 0 & 0 & W_{T_- V_2} & 0 \\ W_{V_1 T_-} & 0 & -W_{T_- V_2} & 0 \\ 0 & 0 & 0 & 0 \end{bmatrix} (\langle n \rangle + 1) \quad (4)$$

and $\langle n \rangle$ the average number of photons in the cavity. The master equation must be solved self-consistently with a photonic balance equation

$$0 = P_{V_1} W_{V_1 T_-} (\langle n \rangle + 1) - P_{V_2} W_{T_- V_2} \langle n \rangle + P_{T_-} [W_{T_- V_2} (\langle n \rangle + 1) - W_{V_1 T_-} \langle n \rangle] - \kappa (\langle n \rangle - \langle n \rangle_{th}) \quad (5)$$

with $\langle n \rangle_{th} = (\exp(\hbar\omega_0/k_B T) - 1)^{-1}$. The photonic transition rates $W_{V_1 T_-}$ and $W_{T_- V_2}$ appearing in the above equations can be expressed as:

$$W_{pq} = \frac{2 |\langle p | h_{so} | q \rangle|^2 \left(\frac{\kappa}{2} + D_{qp} \right)}{(E_p - E_q - 2\pi\hbar\nu_0)^2 + \left(\frac{\kappa}{2} + D_{qp} \right)^2} \quad (6)$$

where κ is the damping rate of the resonator and D_{qp} the decoherence rate associated to the $p \leftrightarrow q$ resonance. The above description is valid provided the transitions $|V_1\rangle \rightarrow |T_-\rangle$ and $|T_-\rangle \rightarrow |V_2\rangle$ are not both resonant with the cavity, i.e. one does not have simultaneously $\delta = 2\Delta_r$ and $2\pi\hbar\nu_0 = \sqrt{2}t_{eh}$. The left inset of Figure 3 shows a zoom on I_{CPS} around $\delta = \delta_l(\nu_0) = 2\Delta_r - 2\pi\hbar\nu_0 + (t_{eh}^2/\pi\hbar\nu_0)$. A current peak occurs at $\delta = \delta_l(\nu_0)$, due to the lasing effect which involves the $|V_1\rangle \rightarrow |T_-\rangle$ transition. Note that the population inversion necessary for the lasing effect is achieved without any AC excitation thanks to the DC bias voltage. The tunnel transition rate from $|T_-\rangle$ to the singly occupied states is larger than the transition rate from $|V_1\rangle$ to the singly occupied states (see Eq.(1)), which explains the increase in I_{CPS} while the system lases. However, for typical parameters, the current peak due to lasing corresponds to ~ 100 fA over a strong background of ~ 10 pA. The lasing effect is more clearly visible through the average number $\langle n \rangle$ of photons in the cavity, which can be measured with microwave amplification techniques [29] (see right inset of figure 3).

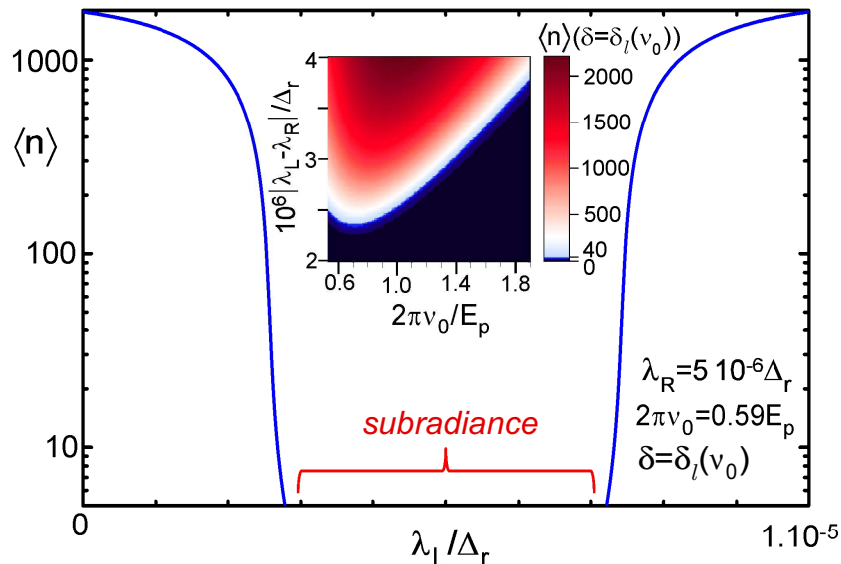


FIG. 4: Main frame: number $\langle n \rangle$ of photons in the cavity for the same parameters as in Figure 3, as a function of the coupling λ_L , for constant values of δ and λ_R . The vanishing of $\langle n \rangle$ for small values of $|\lambda_L - \lambda_R|$ is a direct signature of coherent injection of split Cooper pairs inside the CPS. Inset: maximum number of photons which can be obtained at $\delta = \delta_l(\nu_0)$, as a function of the cavity frequency ν_0 and $|\lambda_L - \lambda_R|$. If $|\lambda_L - \lambda_R|$ is sufficiently large, the lasing effect can be obtained for a broad range of ν_0 .

The peculiar shape of the matrix element (3) is particularly interesting if one can tune independently the couplings $\lambda_{L(R)}$, e.g. tune λ_L while λ_R remains constant (see SM, part F.2). The main frame of Figure 4 shows $\langle n \rangle$ versus λ_L . Strikingly, this curve is not monotonic. When λ_L is too close to λ_R , the average number of photons in the cavity collapses, because the element $\langle T_- | h_{so} | V_n \rangle$ becomes too small. Two lasing thresholds appear, one for $\lambda_L < \lambda_R$ and one for $\lambda_L > \lambda_R$. This non-monotonic behavior is directly due to the presence of the minus signs in Eq.(3) and it therefore represents a smoking gun for coherent Cooper pair injection inside the device. Note that for a typical CPS, the range of cavity frequency ν_0 leading to the lasing effect is rather broad, because the parameter δ can be tuned to $\delta_l(\nu_0)$ with the dots' gate voltages. The inset of figure 4 shows the maximum number of photons in the cavity, obtained at $\delta = \delta_l(\nu_0)$, as a function of ν_0 and $|\lambda_L - \lambda_R|$. For the parameters of Fig. 3 and in particular $|\lambda_L - \lambda_R| = 2.5 \cdot 10^{-6} \Delta_r$, the range $3.3 \text{ GHz} < \nu_0 < 5.9 \text{ GHz}$ allows one to have $\langle n \rangle \geq 40$. Interestingly, for $\delta_r > 2\Delta_r$, the state $|V_2\rangle$ is more probable than $|V_1\rangle$, but it cannot produce any lasing effect. In this case, one can imagine to test the existence of the minus sign in Eq.(3) by applying to the CPS a classical AC gate voltage with frequency $(E_{triplet} - E_2)/2\pi\hbar$ instead of coupling it to the electric field of a cavity. The current through the CPS should show a non-monotonic dependence with respect to λ_L or λ_R . However, the current variations corresponding to this effect might be very small. The lasing effect discussed in this letter presents the advantage of providing an intrinsic and

powerful amplification mechanism for the coefficient $\langle T_- | h_{so} | V_1 \rangle$. This contrasts with a previous proposal where a cavity was not used [30].

Before concluding, we discuss our findings on a more general level. In principle, spin-flip processes induced by the magnetic coupling $g_{L(R)}$ between the cavity photons and spins in dot $L(R)$ can also lead to the subradiance effect. Using a generic single orbital model for each dot, which leads to CPS doubly occupied states $|\sigma, \sigma'\rangle$, we find transition elements between the singlet state $|\downarrow, \uparrow\rangle - |\uparrow, \downarrow\rangle$ and the triplet states $|\uparrow, \uparrow\rangle$ and $|\downarrow, \downarrow\rangle$ which are directly proportional to $g_L - g_R$. This suggests that the subradiance phenomenon studied here is a property of the injected states rather than of the spin/photon coupling mechanism. Nevertheless, in practice, $g_{L(R)}$ is expected to be extremely small [31]. One thus has to consider a spin/photon coupling term mediated by the cavity electric field, like e.g. the term of Eq. (2) caused by spin-orbit coupling. In principle, our findings can be generalized to other types of quantum dots with spin-orbit coupling like InAs quantum dots (see e.g. Ref. [32]), but the detailed analysis of these cases goes beyond the scope of the present work. In our case, we have found a coupling element (3) which vanishes for $\Delta_{K \leftrightarrow K'} = 0$. However, $\Delta_{K \leftrightarrow K'} \neq 0$ is not a fundamental constraint to obtain a subradiant lasing transition. Indeed, at another working point $\delta \sim -2\Delta_r$, we find a third hybridized even state $|V_3\rangle = \sqrt{1-v_3^2}|0, 0\rangle + v_3|\mathcal{S}\rangle$ which can decay radiatively to a triplet state $|T_a\rangle$. One can check that the coupling element $\langle T_a | h_{so} | V_3 \rangle$ has a subradiant form but remains finite for $\Delta_{K \leftrightarrow K'} = 0$. Here, we have chosen to discuss the lasing transition $|V_1\rangle \rightarrow |T_-\rangle$ at $\delta = \delta_l(\nu_0) \sim 2\Delta_r$ because its frequency is more likely to match with the cavity frequency in practice (see SM, section D for details).

In conclusion we have shown that the coherence of entangled states produced by a Cooper pair splitter can be proven by the lasing properties of the device when coupled to a microwave cavity. The idea to probe the coherence of electronic states using the tools of cavity QED could be generalized to many other nanoscale circuits.

We acknowledge fruitful discussions with J. M. Raimond, J. Klinovaja and B. Braunecker. This work was financed by the EU-FP7 project SE2ND[271554].

-
- [1] L. G. Herrmann, F. Portier, P. Roche, A. Levy Yeyati, T. Kontos, and C. Strunk, Phys. Rev. Lett. **104**, 026801 (2010).
 - [2] L. Hofstetter, S. Csonka, J. Nygard, and C. Schönerberger, Nature **461**, 960 (2009).
 - [3] L. Hofstetter, S. Csonka, A. Baumgartner, G. Fülöp, S. d'Hollosy, J. Nygård, C. Schönerberger, Phys. Rev. Lett. **107**, 136801 (2011).
 - [4] T. Martin, Phys. Lett. A **220**, 137 (1996).
 - [5] M. P. Anantram, and S. Datta, Phys. Rev. B **53**, 16390 (1996).
 - [6] G. Burkard, D. Loss, and E. V. Sukhorukov, Phys. Rev. B **61**, 16303 (R) (2000).
 - [7] P. Recher, E. V. Sukhorukov, and D. Loss, Phys. Rev. B **63**, 165314 (2001).
 - [8] G. B. Lesovik, T. Martin, and G. Blatter, Eur. Phys. J. B **24**, 287 (2001).
 - [9] J. Borlin, W. Belzig, and C. Bruder, Phys. Rev. Lett. **88**, 197001 (2002).
 - [10] P. Samuelsson, and M. Büttiker, Phys. Rev. Lett. **89**, 046601 (2002).
 - [11] J. Wei and V. Chandrasekhar, Nature Physics **6**, 494 (2010).
 - [12] J.-M. Raimond, M. Brune, and S. Haroche, Rev. Mod. Phys. **73**, 565 (2001).
 - [13] A. Wallraff, D.I. Schuster, A. Blais, L. Frunzio, R.- S. Huang, J. Majer, S. Kumar, S. M. Girvin, and R. J. Schoelkopf Nature **431**, 162 (2004).
 - [14] M.R. Delbecq, V. Schmitt, F. D. Parmentier, N. Roch, J. J. Viennot, G. Fève, B. Huard, C. Mora, A. Cottet, and T. Kontos arXiv:1108.4371
 - [15] T. Frey, P. J. Leek, M. Beck, A. Blais, T. Ihn, K. Ensslin, and A. Wallraff, arXiv:1108.5378
 - [16] L. Childress, A. S. Sørensen, and M. D. Lukin, Phys. Rev. A **69**, 042302 (2004).
 - [17] A. Cottet, and T. Kontos, Phys. Rev. Lett. **105**, 160502 (2010).
 - [18] A. Cottet, C. Mora, and T. Kontos, Phys. Rev. B **83**, 121311(R) (2011).
 - [19] P.-Q. Jin, M. Marthaler, J. H. Cole, A. Shnirman, and G. Schön, Phys. Rev. B **84**, 035322 (2011).
 - [20] J. Eldridge, M. G. Pala, M. Governale, and J. König, Phys. Rev. B **82**, 184507 (2010).
 - [21] P. Burset, W. J. Herrera, A. Levy Yeyati, Phys. Rev. B **84**, 115448 (2011).
 - [22] T. S. Jespersen, K. Grove-Rasmussen, J. Paaske, K. Muraki, T. Fujisawa, J. Nygård, and K. Flensberg, Nature Physics **7**, 348 (2011).
 - [23] W. Liang, M. Bockrath, and H. Park, Phys. Rev. Lett. **88**, 126801 (2002).
 - [24] F. Kuemmeth, S. Ilani, D. C. Ralph, and P. L. McEuen, Nature **452**, 448 (2008).
 - [25] A. Pályi and G. Burkard, Phys. Rev. Lett. **106**, 086801 (2011).
 - [26] P. Recher, Y. V. Nazarov, and L. P. Kouwenhoven, Phys. Rev. Lett. **104**, 156802 (2010).
 - [27] F. Godschalk, F. Hassler, and Y. V. Nazarov, Phys. Rev. Lett. **107**, 073901 (2011).
 - [28] S. André, V. Brosco, M. Marthaler, A. Shnirman and G. Schön, Phys. Scr., **T137**, 014016 (2009)
 - [29] O. Astafiev, K. Inomata, A. O. Niskanen, T. Yamamoto, Yu. A. Pashkin, Y. Nakamura, and J. S. Tsai, Nature **449**, 588 (2007).

- [30] V. Cerletti, O. Gywat, and D. Loss, Phys. Rev. B **72**, 115316 (2005)
- [31] A. Imamoglu, Phys. Rev. Lett. **102**, 083602 (2010).
- [32] M. Eto and T. Yokoyama, J. Phys. Soc. Jpn. **79**, 123711 (2010).
- [33] W. Izumida, K. Sato, and R. J. Saito, Phys. Soc. Jpn., **78**, 074707 (2009).
- [34] J. Klinovaja, M. J. Schmidt, B. Braunecker, and D. Loss, Phys. Rev. B **84**, 085452 (2011).
- [35] D. Huertas-Hernando, F. Guinea, and A. Brataas, Phys. Rev. B, **74**, 155426 (2006).
- [36] T. Ando, J. Phys. Soc. Jpn. **69**, 1757 (2000).
- [37] A. DeMartino, R. Egger, K. Hallberg, and C. A. Balseiro, Phys. Rev. Lett. **88**, 206402 (2002).
- [38] J.-S. Jeong and H.-W. Lee, Phys. Rev. B **80**, 075409 (2009).
- [39] D. V. Bulaev, B. Trauzettel, and D. Loss, Phys. Rev. B **77**, 235301 (2008).
- [40] Atom-Photon Interactions: Basic Processes and Applications, C. Cohen-Tannoudji, J. Dupont-Roc, G. Grynberg, John Wiley & Sons (1998).
- [41] Quantum noise, C. W. Gardiner, and P. Zoller, Springer, 2004.
- [42] A. Blais, R.-S. Huang, A. Wallraff, S. M. Girvin, and R. J. Schoelkopf, Phys. Rev. A **69**, 062320 (2004).

SUPPLEMENTAL MATERIAL

A. Hamiltonian of the CPS

Inside the left and right dots $i \in \{L, R\}$, an electron with spin $\sigma \in \{\uparrow, \downarrow\}$ can be in the orbital $\tau \in \{K, K'\}$, which is reminiscent from the K/K' degeneracy of graphene. We use a double dot effective hamiltonian which includes the superconducting proximity effect due to the superconducting contact, i.e.

$$H_{ddot}^{eff} = \sum_{i,\tau,\sigma} (\varepsilon + \Delta_{so}\tau\sigma)n_{i\tau\sigma} + H_{int} + \Delta_{K\leftrightarrow K'} \sum_{i,\sigma} (d_{iK\sigma}^\dagger d_{iK'\sigma} + d_{iK'\sigma}^\dagger d_{iK\sigma}) \quad (7)$$

$$+ t_{ee} \sum_{\tau,\sigma} (d_{L\tau\sigma}^\dagger d_{R\tau\sigma} + d_{R\tau\sigma}^\dagger d_{L\tau\sigma}) + t_{eh} \sum_{\tau} \left\{ \left(d_{L\tau\uparrow}^\dagger d_{R\bar{\tau}\downarrow}^\dagger - d_{L\bar{\tau}\downarrow}^\dagger d_{R\tau\uparrow}^\dagger \right) + h.c. \right\}$$

with $\bar{K} = K'$ and $\bar{K}' = K$. The term in t_{eh} accounts for coherent injection of singlet Cooper pairs inside the double dot [20]. Taking into account the superconducting contacts with the term in t_{eh} is valid provided quasiparticle transport between the superconducting contact and the double dot can be disregarded (see part C of the Supplemental Material). For simplicity, we assume that the orbital energies in dots L and R are both equal to ε , which can be obtained by tuning properly the dots' gate voltages. The term H_{int} accounts for Coulomb charging effects. We assume that there cannot be more than one electron in each dot, due to a strong intra-dot Coulomb charging energy. The constant Δ_{so} corresponds to an effective spin-orbit coupling [22]. The term $\Delta_{K\leftrightarrow K'}$ describes a coupling between the K and K' orbitals of dot i , due to disorder at the level of the carbon nanotube atomic structure [22–24]. The hamiltonian H_{ddot}^{eff} must be supplemented by the normal leads hamiltonian $H_{leads} = \sum_{k_\tau, i, \sigma} \varepsilon_{ik_\tau} c_{ik_\tau}^\dagger c_{ik_\tau\sigma} + h.c.$ and the tunnel coupling between the dots and normal leads $H_t = \sum_{k_\tau, \tau, i, \sigma} t c_{ik_\tau}^\dagger d_{i\tau\sigma} + h.c.$, with $c_{ik_\tau\sigma}$ the annihilation operator for an electron with spin σ in orbital k_τ of the normal lead $i \in \{L, R\}$.

B. EXPRESSION OF THE CPS EIGENSTATES

We now discuss the eigenstates and eigenvectors of hamiltonian (7) in the general case. The diagonalization of hamiltonian (7) can be performed by block in five different subspaces, the two subspaces of states occupied with a single spin $\sigma \in \{\uparrow, \downarrow\}$, the two subspaces of states occupied with two equal spins $\sigma \in \{\uparrow, \downarrow\}$, and the subspace comprising the empty state and states occupied with two opposite spins.

B.1. Subspace of singly occupied states with spin σ

One can treat separately the subspace of singly occupied states with spin \uparrow and the subspace of singly occupied states with spin \downarrow . For a given spin direction $\sigma \in \{\uparrow, \downarrow\}$, the eigenenergies and corresponding eigenvectors of H_{ddot}^{eff} are:

eigenenergy	eigenvector
$\varepsilon_{1\sigma} = \varepsilon - t_{ee} - \Delta_r$	$ s_{1\sigma}\rangle = \frac{1}{2}\sqrt{1 - \sigma\frac{\Delta_{so}}{\Delta_r}} (K\sigma, 0\rangle - 0, K\sigma\rangle) + \frac{\Delta_{K/K'}}{2\Delta_r\sqrt{1 - \sigma\frac{\Delta_{so}}{\Delta_r}}} (0, K'\sigma\rangle - K'\sigma, 0\rangle)$
$\varepsilon_{2\sigma} = \varepsilon + t_{ee} - \Delta_r$	$ s_{2\sigma}\rangle = -\frac{1}{2}\sqrt{1 - \sigma\frac{\Delta_{so}}{\Delta_r}} (K\sigma, 0\rangle + 0, K\sigma\rangle) + \frac{\Delta_{K/K'}}{2\Delta_r\sqrt{1 - \sigma\frac{\Delta_{so}}{\Delta_r}}} (0, K'\sigma\rangle + K'\sigma, 0\rangle)$
$\varepsilon_{3\sigma} = \varepsilon - t_{ee} + \Delta_r$	$ s_{3\sigma}\rangle = -\frac{1}{2}\sqrt{1 + \sigma\frac{\Delta_{so}}{\Delta_r}} (K\sigma, 0\rangle - 0, K\sigma\rangle) + \frac{\Delta_{K/K'}}{2\Delta_r\sqrt{1 + \sigma\frac{\Delta_{so}}{\Delta_r}}} (0, K'\sigma\rangle - K'\sigma, 0\rangle)$
$\varepsilon_{4\sigma} = \varepsilon + t_{ee} + \Delta_r$	$ s_{4\sigma}\rangle = \frac{1}{2}\sqrt{1 + \sigma\frac{\Delta_{so}}{\Delta_r}} (K\sigma, 0\rangle + 0, K\sigma\rangle) + \frac{\Delta_{K/K'}}{2\Delta_r\sqrt{1 + \sigma\frac{\Delta_{so}}{\Delta_r}}} (0, K'\sigma\rangle + K'\sigma, 0\rangle)$

with $\Delta_r = \sqrt{\Delta_{so}^2 + \Delta_{K/K'}^2}$. Note that t_{ee} occurs in the expressions of the eigenenergies but not in the expressions of the eigenvectors because we have assumed that the left and rights dot have the same orbital energy ε .

B.2. Subspace of states occupied with two equal spins σ

One can treat separately the subspace of states occupied with two equal spins \uparrow and the subspace of states occupied with two equal spins \downarrow . For a given spin direction $\sigma \in \{\uparrow, \downarrow\}$, the eigenenergies and corresponding eigenvectors of H_{ddot}^{eff} are:

eigenenergy	eigenvector
δ	$ \tilde{S}_{1\sigma}\rangle = \frac{\Delta_{K/K'}}{2\Delta_r} (K'\sigma, K'\sigma\rangle - K\sigma, K\sigma\rangle) + \sigma \frac{\Delta_{so}}{\Delta_r} K'\sigma, K\sigma\rangle$
δ	$ \tilde{S}_{2\sigma}\rangle = \frac{\Delta_{K/K'}}{2\Delta_r} (K'\sigma, K'\sigma\rangle - K\sigma, K\sigma\rangle) + \sigma \frac{\Delta_{so}}{\Delta_r} K\sigma, K'\sigma\rangle$
$\delta - 2\Delta_r$	$ \tilde{S}_{3\sigma}\rangle = \frac{1}{2} \left(\sigma \frac{\Delta_{so}}{\Delta_r} - 1 \right) K\sigma, K\sigma\rangle - \frac{1}{2} \left(1 + \sigma \frac{\Delta_{so}}{\Delta_r} \right) K'\sigma, K'\sigma\rangle + \frac{\Delta_{K/K'}}{2\Delta_r} (K\sigma, K'\sigma\rangle + K'\sigma, K\sigma\rangle)$
$\delta + 2\Delta_r$	$ \tilde{S}_{4\sigma}\rangle = \frac{1}{2} \left(1 + \sigma \frac{\Delta_{so}}{\Delta_r} \right) K\sigma, K\sigma\rangle + \frac{1}{2} \left(1 - \sigma \frac{\Delta_{so}}{\Delta_r} \right) K'\sigma, K'\sigma\rangle + \frac{\Delta_{K/K'}}{2\Delta_r} (K\sigma, K'\sigma\rangle + K'\sigma, K\sigma\rangle)$

with $\tilde{\Delta}_r = \sqrt{\Delta_{so}^2 + (\Delta_{K/K'}^2/2)}$. These states correspond to generalized triplet states with spin 1.

B.3. Subspace of states occupied with two opposite spins

We now discuss the subspace of states comprising the empty state $|0, 0\rangle$ and states occupied with two opposite spins. It is practical to first define the eigenenergies and eigenvectors of H_{ddot}^{eff} for $t_{eh} = 0$:

eigenenergy	eigenvector
0	$ 0, 0\rangle$
δ	$ s_1\rangle = \frac{\Delta_{K/K'}}{2\Delta_r} (\mathcal{C}_-(K \downarrow, K' \uparrow)\rangle - \mathcal{C}_-(K' \downarrow, K \uparrow)\rangle) + \frac{\Delta_{so}}{\Delta_r} \mathcal{C}_-(K' \downarrow, K' \uparrow)\rangle$
δ	$ t_1\rangle = \frac{\Delta_{K/K'}}{2\Delta_r} (\mathcal{C}_+(K \downarrow, K' \uparrow)\rangle - \mathcal{C}_+(K' \downarrow, K \uparrow)\rangle) + \frac{\Delta_{so}}{\Delta_r} \mathcal{C}_+(K' \downarrow, K' \uparrow)\rangle$
δ	$ s_2\rangle = \frac{\Delta_{K/K'}}{2\Delta_r} (\mathcal{C}_-(K \downarrow, K' \uparrow)\rangle - \mathcal{C}_-(K' \downarrow, K \uparrow)\rangle) + \frac{\Delta_{so}}{\Delta_r} \mathcal{C}_-(K \downarrow, K \uparrow)\rangle$
δ	$ t_2\rangle = \frac{\Delta_{K/K'}}{2\Delta_r} (\mathcal{C}_+(K \downarrow, K' \uparrow)\rangle - \mathcal{C}_+(K' \downarrow, K \uparrow)\rangle) + \frac{\Delta_{so}}{\Delta_r} \mathcal{C}_+(K \downarrow, K \uparrow)\rangle$
$\delta - 2\Delta_r$	$2 s_3\rangle = \left(\frac{\Delta_{so}}{\Delta_r} - 1 \right) \mathcal{C}_-(K \uparrow, K' \downarrow)\rangle - \left(\frac{\Delta_{so}}{\Delta_r} + 1 \right) \mathcal{C}_-(K' \uparrow, K \downarrow)\rangle + \frac{\Delta_{K/K'}}{\Delta_r} (\mathcal{C}_-(K \uparrow, K \downarrow)\rangle + \mathcal{C}_-(K' \uparrow, K' \downarrow)\rangle)$
$\delta - 2\Delta_r$	$2 t_3\rangle = \left(\frac{\Delta_{so}}{\Delta_r} - 1 \right) \mathcal{C}_+(K \uparrow, K' \downarrow)\rangle - \left(\frac{\Delta_{so}}{\Delta_r} + 1 \right) \mathcal{C}_+(K' \uparrow, K \downarrow)\rangle + \frac{\Delta_{K/K'}}{\Delta_r} (\mathcal{C}_+(K \uparrow, K \downarrow)\rangle + \mathcal{C}_+(K' \uparrow, K' \downarrow)\rangle)$
$\delta + 2\Delta_r$	$2 s_4\rangle = \left(\frac{\Delta_{so}}{\Delta_r} + 1 \right) \mathcal{C}_-(K \uparrow, K' \downarrow)\rangle + \left(1 - \frac{\Delta_{so}}{\Delta_r} \right) \mathcal{C}_-(K' \uparrow, K \downarrow)\rangle + \frac{\Delta_{K/K'}}{\Delta_r} (\mathcal{C}_-(K \uparrow, K \downarrow)\rangle + \mathcal{C}_-(K' \uparrow, K' \downarrow)\rangle)$
$\delta + 2\Delta_r$	$2 t_4\rangle = \left(\frac{\Delta_{so}}{\Delta_r} + 1 \right) \mathcal{C}_+(K \uparrow, K' \downarrow)\rangle + \left(1 - \frac{\Delta_{so}}{\Delta_r} \right) \mathcal{C}_+(K' \uparrow, K \downarrow)\rangle + \frac{\Delta_{K/K'}}{\Delta_r} (\mathcal{C}_+(K \uparrow, K \downarrow)\rangle + \mathcal{C}_+(K' \uparrow, K' \downarrow)\rangle)$

where $|\mathcal{C}_{\pm}(\tau\sigma, \tau'\sigma')\rangle = (|\tau\sigma, \tau'\sigma'\rangle \pm |\tau'\sigma', \tau\sigma\rangle)/\sqrt{2}$. From the definition of $|\mathcal{C}_{\pm}(\tau\sigma, \tau'\sigma')\rangle$, one can view the states $|s_1\rangle$, $|s_2\rangle$, $|s_3\rangle$ and $|s_4\rangle$ as generalized singlet states whereas $|t_1\rangle$, $|t_2\rangle$, $|t_3\rangle$ and $|t_4\rangle$ can be viewed as generalized triplet states with total spin 0. In the subspace $\{|0, 0\rangle, |s_1\rangle, |t_1\rangle, |s_2\rangle, |t_2\rangle, |s_3\rangle, |t_3\rangle, |s_4\rangle, |t_4\rangle\}$, the hamiltonian (7) writes exactly:

$$\begin{aligned} \tilde{H}_{ddot}^{eff} = & \delta(|s_1\rangle\langle s_1| + |s_2\rangle\langle s_2| + |t_1\rangle\langle t_1| + |t_2\rangle\langle t_2|) + (\delta - 2\Delta_r)(|t_3\rangle\langle t_3| + |s_3\rangle\langle s_3|) + (\delta + 2\Delta_r)(|t_4\rangle\langle t_4| + |s_4\rangle\langle s_4|) \\ & + \sqrt{2}t_{eh}(|s_4\rangle\langle 0, 0| + |0, 0\rangle\langle s_4| - |s_3\rangle\langle 0, 0| - |0, 0\rangle\langle s_3|) \end{aligned}$$

Thus, the states $|s_1\rangle$, $|s_2\rangle$, $|t_1\rangle, |t_2\rangle$, $|t_3\rangle$ and $|t_4\rangle$ are eigenstates of H_{ddot}^{eff} while the states $|s_3\rangle$, and $|s_4\rangle$ and are hybridized with $|0, 0\rangle$. This hybridization leads to three eigenstates $|V_1\rangle$, $|V_2\rangle$ and $|V_3\rangle$ with energy E_1 , E_2 and E_3 . Figure 1 shows the energy of the different doubly occupied eigenstates (with total spin 1 or 0, i.e. given by sections B.2 or B.3) as a function of δ . The triplet states have energies δ , $\delta - 2\Delta_r$ or $\delta + 2\Delta_r$ (blue lines), while the energies E_1 , E_2 and E_3 (red, green and pink lines) show two anticrossings at $\delta = -2\Delta_r$ and $\delta = 2\Delta_r$.

B.4. Expression of the CPS doubly occupied eigenstates for $\delta \sim 2\Delta_r$

In the main text, we work near the right anticrossing in Figure 1 ($\delta \sim 2\Delta_r$). For $\delta \sim 2\Delta_r$, a simplified expression of the relevant doubly occupied eigenstates of H_{ddot}^{eff} can be obtained by performing a diagonalization in the subspace

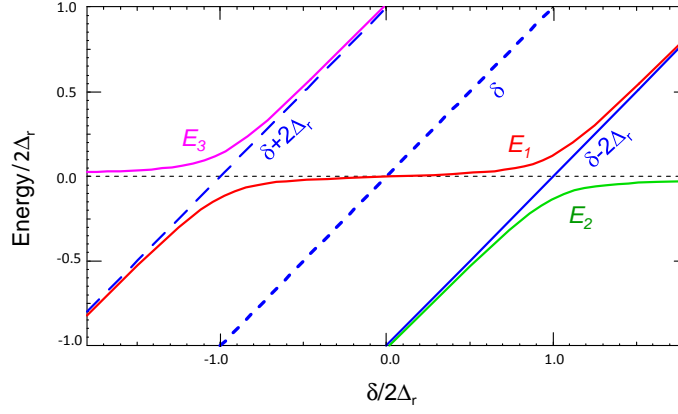


FIG. 5: Energy of the different doubly occupied eigenstates (with total spin 0 or 1) as a function of δ .

$\{|0, 0\rangle, |s_3\rangle, |t_3\rangle, |\tilde{S}_{3\uparrow}\rangle, |\tilde{S}_{3\downarrow}\rangle\}$. This leads to the CPS eigenstates $|V_1\rangle, |V_2\rangle, |T_0\rangle, |T_+\rangle$ and $|T_-\rangle$ discussed in the main text, which are defined by:

eigenenergy	eigenvector
$\delta - 2\Delta_r$	$ T_0\rangle = t_3\rangle = \sum_{\sigma} \left\{ \frac{1}{2}(\sigma \frac{\Delta_{so}}{\Delta_r} - 1) \mathcal{C}_+(K\sigma, K'\bar{\sigma})\rangle \right\} + \frac{\Delta_{K/K'}}{2\Delta_r} \sum_{\tau} \mathcal{C}_+(\tau \uparrow, \tau \downarrow)\rangle$
$\delta - 2\Delta_r$	$ T_+\rangle = \frac{ \tilde{S}_{3\uparrow}\rangle - \tilde{S}_{3\downarrow}\rangle}{\sqrt{2}} = \sum_{\sigma} \left\{ \frac{1}{2} \left(\frac{\Delta_{so}}{\Delta_r} - \sigma \right) \frac{ K\sigma, K\sigma\rangle - K'\bar{\sigma}, K'\bar{\sigma}\rangle}{\sqrt{2}} + \sigma \frac{\Delta_{K/K'}}{2\Delta_r} \mathcal{C}_+(K\sigma, K'\sigma)\rangle \right\}$
$\delta - 2\Delta_r$	$ T_-\rangle = \frac{ \tilde{S}_{3\uparrow}\rangle + \tilde{S}_{3\downarrow}\rangle}{\sqrt{2}} = \sum_{\sigma} \left\{ \frac{1}{2} \left(\frac{\Delta_{so}}{\Delta_r} \sigma - 1 \right) \frac{ K\sigma, K\sigma\rangle + K'\bar{\sigma}, K'\bar{\sigma}\rangle}{\sqrt{2}} + \frac{\Delta_{K/K'}}{2\Delta_r} \mathcal{C}_+(K\sigma, K'\sigma)\rangle \right\}$
E_1	$ V_1\rangle = \sqrt{1 - v_1^2} 0, 0\rangle + v_1 \mathcal{S}\rangle$
E_2	$ V_2\rangle = \sqrt{1 - v_2^2} 0, 0\rangle + v_2 \mathcal{S}\rangle$

with

$$E_i = \frac{1}{2} \left(\delta - 2\Delta_r - (-1)^n \sqrt{8t_{eh}^2 + (\delta - 2\Delta_r)^2} \right)$$

$$v_n = \frac{2t_{eh}}{\sqrt{8t_{eh}^2 + (\delta - 2\Delta_r)(\delta - 2\Delta_r + (-1)^n \sqrt{8t_{eh}^2 + (\delta - 2\Delta_r)^2})}}$$

and

$$|\mathcal{S}\rangle = |s_3\rangle = \sum_{\sigma} \left\{ \frac{1}{2} \left(\frac{\Delta_{so}}{\Delta_r} - \sigma \right) |\mathcal{C}_-(K\sigma, K'\bar{\sigma})\rangle \right\} + \frac{\Delta_{K/K'}}{2\Delta_r} \sum_{\tau} |\mathcal{C}_-(\tau \uparrow, \tau \downarrow)\rangle$$

Note that $\sigma = \pm 1$ stands for $\sigma \in \{\uparrow, \downarrow\}$ in algebraic expressions. The state $|T_0\rangle$ corresponds to a generalized triplet state with zero spin, $|T_-\rangle$ and $|T_+\rangle$ correspond to a coherent mixture of two triplet states with finite spin, and the state $|\mathcal{S}\rangle$ corresponds to a generalized spin-singlet state. Note that without disorder ($\Delta_{K \leftrightarrow K'} = 0$), $|\mathcal{S}\rangle$ has components in $|\mathcal{C}_+(\tau \downarrow, \bar{\tau} \uparrow)\rangle$ only and $|T_-\rangle$ has components in $|\tau\sigma, \tau\sigma\rangle$ only. In the presence of disorder, $|\mathcal{S}\rangle$ also includes components in $|\mathcal{C}_-(\tau \uparrow, \tau \downarrow)\rangle$, and $|T_-\rangle$ has also components in $|K\sigma, K'\sigma\rangle$ and $|K'\sigma, K\sigma\rangle$. This enables a coupling between the states $|V_{1(2)}\rangle$ and $|T_-\rangle$ through H_{so} .

C. BIAS VOLTAGE WINDOW

The hamiltonian H_{ddot}^{eff} can be used provided there is no quasiparticle transport between the superconducting lead and the dots. This requires

$$-\Delta < -eV < \Delta \quad (8)$$

In the main text, we furthermore assume that electrons can go from the double dot to the normal metal leads but not the reverse. This is true provided the bias voltage V belongs to a certain range which we derive below.

(1) We recall that the double dot singly occupied states $|s_{i\sigma}\rangle$ have energies $\varepsilon_{i\sigma}$, with $i \in \{1, 2, 3, 4\}$, given in section B.1 of the supplemental material. We assume $\delta \sim 2\Delta_r$, so that the states $|V_1\rangle$ and $|V_2\rangle$ have significant components in $|0, 0\rangle$ and $|\mathcal{S}\rangle$ and their energies E_1 and E_2 are well approximated by the expressions given in section B.4. Since $|V_1\rangle$ and $|V_2\rangle$ have components in $|\mathcal{S}\rangle$, they can decay towards the singly occupied state $|s_{i\sigma}\rangle$ while an electron is transferred to the normal metal leads (and the reverse process is forbidden) if

$$-eV < E_{1(2)} - \varepsilon_{i\sigma} - \alpha k_B T \quad (9)$$

for $i \in \{1, 2, 3, 4\}$. Above, α is a dimensionless factor of order 1 which takes into account the temperature broadening of the levels.

(2) Since $|V_1\rangle$ and $|V_2\rangle$ have also components in $|0, 0\rangle$, a singly occupied state can decay towards $|V_1\rangle$ or $|V_2\rangle$ while an electron is transferred to the normal leads (and the reverse process is forbidden) if

$$-eV < \varepsilon_{i\sigma} - E_{1(2)} - \alpha k_B T \quad (10)$$

for $i \in \{1, 2, 3, 4\}$.

(3) Since we assume $\delta \sim 2\Delta_r$, the state $|V_3\rangle$ has a negligible component in $|0, 0\rangle$. Hence, it can be considered as a pure doubly occupied state, with energy $E_3 \simeq \delta + 2\Delta$. The other doubly occupied states have energies $\delta - 2\Delta_r$, $\delta + 2\Delta_r$, or δ (see section B.2 and B.3). The doubly occupied states (including $|V_3\rangle$) can relax to the singly occupied state $|s_{i\sigma}\rangle$ while an electron is transferred to the normal leads (and the reverse processes are forbidden) if

$$-eV < \delta \pm 2\Delta_r - \varepsilon_{i\sigma} - \alpha k_B T \quad (11)$$

and

$$-eV < \delta - \varepsilon_{i\sigma} - \alpha k_B T \quad (12)$$

Since $E_2 < \delta - 2\Delta_r < E_1$, $\delta < \delta + 2\Delta_r < E_3$ and $\varepsilon_{1\sigma} < \varepsilon_{2\sigma}, \varepsilon_{3\sigma} < \varepsilon_{4\sigma}$, the combination of Eqs. (8), (9), (10), (11) and (12) yields the constraint

$$-\Delta < -eV < \min(E_2 - \varepsilon_{4\sigma}, \varepsilon_{1\sigma} - E_1) - \alpha k_B T$$

We note $\delta = 2\varepsilon$. For $\delta \sim 2\Delta_r$, one has

$$E_2 - \varepsilon_{4\sigma} = -2\Delta_r - t_{ee} - \frac{1}{2}\sqrt{8t_{eh}^2 + (\delta - 2\Delta_r)^2} = \varepsilon_{1\sigma} - E_1 - 2\Delta_r$$

We conclude that we have to satisfy

$$-\Delta < -eV < -2\Delta_r - t_{ee} - \frac{1}{2}\sqrt{8t_{eh}^2 + (\delta - 2\Delta_r)^2} - \alpha k_B T$$

with Δ the BCS gap of the superconducting contact. Since the temperature T is much smaller than Δ_r in a typical experiment, we simplify this criterion as

$$-\Delta < -eV < -2\Delta_r - t_{ee} - \frac{1}{2}\sqrt{8t_{eh}^2 + (\delta - 2\Delta_r)^2}$$

With the parameters of Fig.2, $t_{ee} \ll \Delta_r$, $\delta \sim 2\Delta_r$ and Δ the BCS gap of NbN, this gives $1.8 \text{ meV} \lesssim eV \lesssim 3 \text{ meV}$.

To populate the state $|V_3\rangle$ and the triplet states other than $|T_-\rangle$, one needs to have a transition from a singly occupied state to one of these states. In the regime we consider above, this is not possible since this would require an electron to go from the normal metal leads to the double dot. Therefore, the state $|V_3\rangle$ and the triplet states other than $|T_-\rangle$ are not active. In contrast, the state $|T_-\rangle$ can be populated due to lasing transitions $|V_1\rangle \rightarrow |T_-\rangle$.

D. EFFECT OF THE SPIN-ORBIT COUPLING

In order to discuss the effect of the term h_{so} appearing in Eq. (2) of the main text, it is practical to redefine the eigenvectors of H_{ddot}^{eff} in the subspace of states occupied with two equal spins as

eigenenergy	eigenvectors
δ	$ T_a\rangle = \frac{\alpha_+}{\sqrt{\alpha_-^2 + \alpha_+^2}} \frac{ \tilde{S}_{1\uparrow}\rangle - \tilde{S}_{2\downarrow}\rangle}{\sqrt{2}} - \frac{\alpha_-}{\sqrt{\alpha_-^2 + \alpha_+^2}} \frac{ \tilde{S}_{2\uparrow}\rangle - \tilde{S}_{1\downarrow}\rangle}{\sqrt{2}}$
δ	$ T_b\rangle = \frac{\alpha_-}{\sqrt{\alpha_-^2 + \alpha_+^2}} \frac{ \tilde{S}_{1\uparrow}\rangle - \tilde{S}_{2\downarrow}\rangle}{\sqrt{2}} - \frac{\alpha_+}{\sqrt{\alpha_-^2 + \alpha_+^2}} \frac{ \tilde{S}_{2\uparrow}\rangle - \tilde{S}_{1\downarrow}\rangle}{\sqrt{2}}$
δ	$ T_{1-}\rangle = \frac{ \tilde{S}_{1\uparrow}\rangle + \tilde{S}_{2\downarrow}\rangle}{\sqrt{2}}$
δ	$ T_{2-}\rangle = \frac{ \tilde{S}_{2\uparrow}\rangle + \tilde{S}_{1\downarrow}\rangle}{\sqrt{2}}$
$\delta - 2\Delta_r$	$ T_+\rangle$ already defined in section B.4
$\delta - 2\Delta_r$	$ T_-\rangle$ already defined in section B.4
$\delta + 2\Delta_r$	$ \tilde{S}_{4\uparrow}\rangle$
$\delta + 2\Delta_r$	$ \tilde{S}_{4\downarrow}\rangle$

with

$$\alpha_{\mp} = \lambda_L - \lambda_R \mp \frac{\Delta_{so}}{\Delta_r} (\lambda_L + \lambda_R)$$

For $\delta \sim 2\Delta_r$ and the bias voltage conditions considered in section C, the states $|V_1\rangle$ and $|V_2\rangle$ can be populated but not $|V_3\rangle$. Only two of the triplet states, namely $|T_-\rangle$ and $|T_b\rangle$, are coupled to $|V_1\rangle$ and $|V_2\rangle$ by h_{so} . One has

$$\langle T_-\rangle |h_{so}|V_{1(2)}\rangle = \mathbf{i}v_{1(2)} \frac{\Delta_{K\leftrightarrow K'}}{\Delta_r} (\lambda_L - \lambda_R) \quad (13)$$

which corresponds to Eq. (3) of the main text, and

$$\langle T_b | h_{so} | V_{1(2)} \rangle = \frac{\mathbf{i}v_{1(2)} \Delta_{so}^2 (\lambda_R^2 - \lambda_L^2)}{\sqrt{\tilde{\Delta}_r \left(\Delta_{so}^2 (\lambda_L^2 + \lambda_R^2) + \frac{\Delta_{K/K'}^2}{2} (\lambda_L - \lambda_R)^2 \right)}} \quad (14)$$

The couplings to $|T_-\rangle$ and $|T_b\rangle$ are both subradiant since they vanish for $\lambda_L = \lambda_R$. For $\Delta_{K\leftrightarrow K'} = 0$, the coupling between $|T_-\rangle$ and $|V_{1(2)}\rangle$ vanishes, whereas the coupling between $|T_b\rangle$ and $|V_{1(2)}\rangle$ persists:

$$\lim_{\Delta_{K\leftrightarrow K'} \rightarrow 0} \langle T_b | h_{so} | V_{1(2)} \rangle = \frac{\mathbf{i}v_{1(2)} (\lambda_R^2 - \lambda_L^2)}{\sqrt{\lambda_L^2 + \lambda_R^2}} \quad (15)$$

We conclude that it is not necessary to use a finite $\Delta_{K\leftrightarrow K'}$ to obtain a coupling between $|V_{1(2)}\rangle$ and a triplet state. It is nevertheless impossible to use the transitions $|V_{1(2)}\rangle \leftrightarrow |T_b\rangle$ for lasing since $|T_b\rangle$ is higher in energy than $|V_1\rangle$ and $|V_2\rangle$.

For $\delta \sim -2\Delta_r$, the state $|V_3\rangle$ can be populated. When $\Delta_{K\leftrightarrow K'} = 0$, we find that only one of the triplet states, namely $|T_a\rangle$, is coupled to $|V_3\rangle$, with a coupling element

$$\lim_{\Delta_{K\leftrightarrow K'} \rightarrow 0} \langle T_a | h_{so} | V_3 \rangle = \frac{\mathbf{i}v_3 (\lambda_R^2 - \lambda_L^2)}{\sqrt{\lambda_L^2 + \lambda_R^2}} \quad (16)$$

When $\Delta_{K\leftrightarrow K'} \neq 0$, one has:

$$\langle T_a | h_{so} | V_3 \rangle = \frac{\mathbf{i}v_3 \Delta_{so}^2 (\lambda_R^2 - \lambda_L^2)}{\sqrt{\tilde{\Delta}_r \left(\Delta_{so}^2 (\lambda_L^2 + \lambda_R^2) + \frac{\Delta_{K/K'}^2}{2} (\lambda_L - \lambda_R)^2 \right)}} \quad (17)$$

These equations are analogue to Eqs. (15) and (14). In principle, if the cavity frequency is matching with $E_3 - \delta \sim 2\Delta_r + \sqrt{2}t_{eh}$, there can be lasing transitions from $|V_3\rangle$ to $|T_a\rangle$ since $|V_3\rangle$ is higher in energy than $|T_a\rangle$. The $|V_3\rangle \leftrightarrow |T_a\rangle$ transitions are subradiant since $\langle T_a | h_{so} | V_3 \rangle$ cancels for $\lambda_L = \lambda_R$. Importantly, $\langle T_a | h_{so} | V_3 \rangle$ remains finite for $\Delta_{K \leftrightarrow K'} = 0$. Therefore, $\Delta_{K \leftrightarrow K'} \neq 0$ is not a fundamental constraint to obtain a subradiant lasing transition in our system. Nevertheless, in practice, the frequency of the $|V_3\rangle \leftrightarrow |T_a\rangle$ transition is not likely to match with the cavity frequency because $\Delta_{K/K'}, \Delta_{so} \gg 2\pi\nu_0$ is expected [22, 24]. We have chosen to discuss the lasing transition $|V_1\rangle \leftrightarrow |T_- \rangle$ at $\delta \sim 2\Delta_r$ because it corresponds to a frequency of the order of $\sqrt{2}t_{eh}$, which is expected to be much smaller [1].

E. OTHER POSSIBLE LASING TRANSITIONS

- In principle, there can be radiative transitions from $|T_- \rangle$ to $|V_2\rangle$, which are taken into account by Eq.(7) of the main text. However, the lasing threshold corresponding to this transition is not reached in the regime of parameters we consider, because the population of state $|T_- \rangle$ is negligible for $\delta > 2\Delta_r$.
- Since the parameter δ depends on the dots' gate voltages, cavity photons can also couple to the CPS through the operator $\hat{\delta}_{diff} = \sum_{\tau, \sigma, \tau', \sigma'} |\tau\sigma, \tau'\sigma'\rangle \langle \tau\sigma, \tau'\sigma'|$. One finds $\langle V_1 | \hat{\delta}_{diff} | V_2 \rangle = \sqrt{2}t_{eh} / \sqrt{8t_{eh}^2 + (\delta - 2\Delta_r)^2}$. Hence, in principle, there can be lasing between the states $|V_1\rangle$ and $|V_2\rangle$. Nevertheless, this can be avoided by using $E_0 = 2\pi\hbar\nu_0 < 2\sqrt{2}t_{eh}$ or by tuning properly δ , so that $E_0 \neq E_1 - E_2$.
- In principle, spin-orbit interaction can also induce lasing transitions inside the CPS singly occupied charge sector, corresponding to energy differences $2\Delta_r$, $2\Delta_r + 2t_{ee}$, $2\Delta_r - 2t_{ee}$ and $2t_{ee}$. Since the scale Δ_r is expected to be much larger than E_0 , only the transitions with frequency $t_{ee}/\pi\hbar$ can possibly match with the cavity frequency ν_0 . However, it is rather unlikely to have such a matching in practice. In the main text we assume $\nu_0 \neq t_{ee}/\pi\hbar$. This criterion can be checked experimentally by extracting t_{ee} from the data.

F. EVALUATION OF THE SPIN/PHOTON COUPLING IN A CARBON-NANOTUBE BASED QUANTUM DOT

In this section, we estimate the spin/photon coupling $\lambda_{L(R)}$ which can be obtained in the single-wall carbon-nanotube based quantum dot $L(R)$ thanks to spin-orbit coupling.

F.1. Electronic wavefunction in the absence of inter-subband coupling elements

The position \vec{u} of an electron on the nanotube is marked with a longitudinal coordinate ξ and an azimuthal angle φ , i.e. $\vec{u} = \xi \vec{z} + R \cos[\varphi] \vec{x} + R \sin[\varphi] \vec{y}$ with R the nanotube radius. We write electronic wavevectors under the form

$$|\Psi\rangle = e^{i\kappa\varphi} |\psi\rangle \otimes |\sigma\rangle \quad (18)$$

where κ is the electronic circumferential wavevector, $|\sigma\rangle$ denotes the spin part of the wavefunction and $|\psi\rangle$ is the ξ -dependent orbital part, which has a structure in sublattice space. We use the spin index $\sigma \in \{\uparrow, \downarrow\}$ and the sublattice index $\tau \in \{K, K'\}$ or equivalently $\sigma \in \{+, -\}$ and $\tau \in \{+, -\}$ in algebraic expressions. For a zigzag nanotube, $\langle \xi | \varphi \rangle$ is an eigenvector of

$$H_{SWNT} = \hbar v(\tau\kappa s_1 - is_2 \frac{\partial}{\partial \xi}) + \sigma\tau\Delta_{so}^0 s_0 + \sigma\tau\Delta_{so}^1 s_1 - \Delta_g s_1 + V(\xi)s_0$$

with $V(\xi)$ a longitudinal confinement potential and $\{s_0, s_1, s_2, s_3\}$ the identity and Pauli operators in sublattice space. We have used the same conventions as in Refs. [22, 39] to write H_{SWNT} . The motion of electrons along the nanotube circumference is quantized, i.e.

$$\kappa = (N + \frac{\tau\eta}{3}) \frac{1}{R}$$

with N the subband index and $\eta \in \{-1, 0, 1\}$ a parameter which depends on the nanotube chiral vector. We have introduced in the above hamiltonian intra-subband spin-orbit coupling terms in Δ_{so}^1 , Δ_{so}^0 and a spin-independent term in Δ_g , which are derived e.g. in Refs. [33, 34]. The constants Δ_{so}^1 and Δ_{so}^0 are first order in the atomic spin-orbit interaction V_{so} and the nanotube curvature R^{-1} , whereas Δ_g is proportional to R^{-2} .

For a problem uniform in the ξ direction ($V(\xi) = 0$), the eigenstates $|\psi\rangle = |\psi_{\tau,N,k,\sigma}^0\rangle$ of the above hamiltonian satisfy $H_{SWNT} |\psi_{\tau,N,k,\sigma}^0\rangle = E_{\tau,N,k,\sigma} |\psi_{\tau,N,k,\sigma}^0\rangle$, with k the electrons longitudinal wavevector. One can check:

$$\langle \xi | \psi_{\tau,N,k,\sigma}^0 \rangle = \begin{pmatrix} u_{\tau,N,k,\sigma} \\ 1 \end{pmatrix} e^{ik\xi} = \begin{pmatrix} b \frac{\hbar v_F \tau \kappa + \sigma \tau \Delta_{so}^1 - \Delta_g - i \hbar v_F k}{\sqrt{(\hbar v_F \tau \kappa + \sigma \tau \Delta_{so}^1 - \Delta_g)^2 + (\hbar v_F k)^2}} \\ 1 \end{pmatrix} e^{ik\xi}$$

and

$$E_{\tau,N,k,\sigma} = \sigma \tau \Delta_{so}^0 + b \sqrt{(\hbar v_F \tau \kappa + \sigma \tau \Delta_{so}^1 - \Delta_g)^2 + (\hbar v_F k)^2} \quad (19)$$

with $b = \pm 1$ for the conduction/valence band. In the following, we use $b = 1$. In order to define a quantum dot, we take into account a rectangular confinement potential

$$V(\xi) = \begin{cases} V_{conf} & \text{for } \xi < 0 \\ 0 & \text{for } 0 < \xi < L \\ V_{conf} & \text{for } \xi > L \end{cases}$$

We obtain confined electronic states $|\psi\rangle = |\Psi_{\tau,N,n,\sigma}\rangle$, with n the index corresponding to a longitudinal confinement of electrons. More precisely, one has

$$\langle \xi | \psi_{\tau,N,n,\sigma} \rangle = \begin{cases} \frac{A_{\tau,N,n,\sigma}}{\sqrt{2\pi}} e^{\tilde{k}_1^n \xi} \begin{pmatrix} u_{\tau,N,-i\tilde{k}_1^n,\sigma} \\ 1 \end{pmatrix} & \text{for } \xi < 0 \\ \frac{C_{\tau,N,n,\sigma}}{\sqrt{2\pi}} e^{ik_1^n \xi} \begin{pmatrix} u_{\tau,N,k_1^n,\sigma} \\ 1 \end{pmatrix} + \frac{D_{\tau,N,n,\sigma}}{\sqrt{2\pi}} e^{-ik_1^n \xi} \begin{pmatrix} u_{\tau,N,-k_1^n,\sigma} \\ 1 \end{pmatrix} & \text{for } 0 < \xi < L \\ \frac{B_{\tau,N,n,\sigma}}{\sqrt{2\pi}} e^{\tilde{k}_1^n (L-\xi)} \begin{pmatrix} u_{\tau,N,i\tilde{k}_1^n,\sigma} \\ 1 \end{pmatrix} & \text{for } \xi > L \end{cases}$$

with $k_1^n > 0$ and $\text{Re}[\tilde{k}_1^n] > 0$. The wavevectors k_1^n and \tilde{k}_1^n can be obtained from the energy-conservation condition

$$E_{\tau,N,k_1^n,\sigma} = E_{\tau,N,-i\tilde{k}_1^n,\sigma} + V_{conf} \quad (20)$$

the constraint

$$n \frac{\pi}{L} < k_1^n < (n+1) \frac{\pi}{L}$$

and the secular condition

$$\exp(i2k_1^n L) = \frac{\left(u_{\tau,N,i\tilde{k}_1^n,\sigma} - u_{\tau,N,-k_1^n,\sigma} \right) \left(u_{\tau,N,-i\tilde{k}_1^n,\sigma} - u_{\tau,N,k_1^n,\sigma} \right)}{\left(u_{\tau,N,-i\tilde{k}_1^n,\sigma} - u_{\tau,N,-k_1^n,\sigma} \right) \left(u_{\tau,N,i\tilde{k}_1^n,\sigma} - u_{\tau,N,k_1^n,\sigma} \right)}$$

which results from the continuity of $|\psi_{\tau,N,n,\sigma}\rangle$ at $\xi = 0$ and $\xi = L$. The constants $A_{\tau,N,n,\sigma}$, $B_{\tau,N,n,\sigma}$, $C_{\tau,N,n,\sigma}$, and $D_{\tau,N,n,\sigma}$ can be obtained from the continuity of $|\psi_{\tau,N,n,\sigma}\rangle$ and its normalization condition, i.e. $\int_{-\infty}^{\infty} d\xi |\langle \psi_{\tau,N,n,\sigma} | \psi_{\tau,N,n,\sigma} \rangle|^2 = 1$.

F.2. Effect of the inter-subband coupling elements

In this section, we discuss the coupling between electronic spins and cavity photons, mediated by the electromagnetic field of the cavity.

- We assume that the nanotube is parallel to the cavity central conductor. We take into account the interaction of electrons with the vector potential \vec{A} of the cavity treated in the Coulomb gauge [39, 40]. We quantize the field \vec{A} in terms of the photonic operators[41, 42]. This gives a coupling operator

$$H_{inter}^A = -\frac{e\hbar V_{rms}}{8\pi m_{eff} R \nu_0 d} (a + a^\dagger) [(\mu_+ - \mu_-) \frac{\partial}{\partial \varphi} + \frac{\partial}{\partial \varphi} (\mu_+ - \mu_-)]$$

We have used above $\sin(\varphi) = (\mu_+ - \mu_-)/2i$, where the operator $\mu_\pm = e^{\pm i\varphi}$ increases/decreases the index N .

- The subband and spin subspaces are coupled by a term [33, 34]

$$H_{inter}^{so} = -\Delta_{so}^1 s_2 i (\sigma_- \mu_+ - \sigma_+ \mu_-)$$

which is first order in the atomic spin-orbit interaction V_{so} and the nanotube curvature R^{-1} (spin-orbit interaction in carbon nanotubes was also discussed in Refs. 35–39). Here, σ_\pm is the operator increasing/decreasing the spin index in $|\sigma\rangle$.

- Note that the terms H_{inter}^A and H_{inter}^{so} apply to the full wavefunctions [see Eq. (18)]

$$|\Psi_{\tau, N, n, \sigma}\rangle = e^{i(N + \frac{\tau n}{3})\varphi} |\psi_{\tau, N, n, \sigma}\rangle \otimes |\sigma\rangle$$

One can perform a first order perturbation of these wavefunctions by H_{inter}^{so} :

$$|\tilde{\Psi}_{\tau, N, n, \sigma}\rangle = |\Psi_{\tau, N, n, \sigma}\rangle + \sum_{n'} \lambda_{\tau, N, n, n'}^{-\sigma} |\Psi_{\tau, N + \sigma, n', -\sigma}\rangle$$

with

$$\lambda_{\eta, \tau, N, n, n'}^\sigma = \frac{\langle \Psi_{\tau, N - \sigma, n', \sigma} | H_{inter}^{so} | \Psi_{\tau, N, n, -\sigma} \rangle}{E_{\tau, N, n, -\sigma} - E_{\tau, N - \sigma, n', \sigma}}$$

- The term H_{inter}^A couples the perturbed wavefunctions $|\tilde{\Psi}_{\tau, N, n, \sigma}\rangle$ for $\sigma = \uparrow$ and $\sigma = \downarrow$. This yields intra-subband spin/photon coupling elements, which write for the lower subband $N = 0$ which we consider:

$$\begin{aligned} \lambda_\tau &= \left\langle \tilde{\Psi}_{\tau, N=0, n, -1}(\vec{r}) \left| H_{inter}^A \right| \tilde{\Psi}_{\tau, N=0, n, +1}(\vec{r}) \right\rangle \\ &= P \left(\frac{\tau \eta}{3} \left(\lambda_{\tau, N=0, n, n}^- + \lambda_{\tau, N=0, n, n}^+ \right) + \frac{1}{2} \left(\lambda_{\tau, N=0, n, n}^- - \lambda_{\tau, N=0, n, n}^+ \right) \right) \end{aligned}$$

with $P = ie\hbar V_{rms}/8\pi m_{eff} R \nu_0 d$.

- One can check that $\lambda_K = \lambda_{K'} = -i\lambda$ is purely imaginary due to the assumptions used above [zigzag nanotube and $V(\xi - \frac{L}{2}) = V(\frac{L}{2} - \xi)$]. One thus obtains the intra-subband spin/photon coupling term of Eq.(3) of the main text. For $L = 100$ nm, $R = 1$ nm, $\eta = 1$, $d = 5$ μ m, $V_{rms} = 4$ μ V, $\nu_0 = 3.64$ GHz, $E_{conf} = \hbar v_F/3R$, $m_{eff} = \hbar |\kappa|/v_F = 4.4 \cdot 10^{-32}$ kg, and using the parameters $\Delta_{so}^1 = -0.08$ meV, $\Delta_{so}^0 = -0.32$ meV, and $\Delta_g = 5.7$ meV taken from Ref. 34, we obtain $\lambda \simeq 0.4$ MHz.
- In order to obtain a tunable spin/photon coupling, one can insert in one of the dots gate voltage supply a tunable capacitance made out of a single electron transistor (SET). The electric field seen by the nanotube can be modulated electrostatically by placing the SET in the blockaded or transporting regimes. This allows one to vary the couplings $\lambda_{L(R)}$ for dot $L(R)$.
- In the case $\lambda_{iK} \neq \lambda_{iK'}$, with i the dot index added in the main text, the results of the main text can be generalized straightforwardly by using

$$\langle T_- | h_{so} | V_n \rangle = v_n \frac{\Delta_{K \leftrightarrow K'}}{2\Delta_r} (\lambda_{LK} + \lambda_{LK'} - \lambda_{RK} - \lambda_{RK'}) \quad (21)$$